Image Processing, Electronics and Computers
L. Trajkovic et al. (Eds.)

doi:10.3233/ATDE240467

Non-Line-of-Sight Target Localization Based on Multipath Exploitation

Kai WEN[a], Yishuo WU[a,1] and Khalid YAHYA[b]
[a] *School of Communications and Information Engineering, Chongqing University of Posts and Telecommunications, Chongqing 400065, China*
[b] *Istanbaul Gelisim University, Istanbul, Turkey*

Abstract. Detecting targets located in non-line-of-sight (NLOS) areas within urban environments has attracted widespread attention in recent years. However, imaging localization algorithms based on multipath superposition often generate false target points, leading to interference in target location acquisition. This article proposes a new multi-target localization method specifically designed for L-shaped building scenarios without producing target ghosting, by studying the correlation between times of arrival (TOAs) and multipath types. Specifically, the propagation mode of the signal is first analyzed to construct a multipath echo model. The principle of specular reflection is utilized to introduce virtual radars, and virtual radar coordinates corresponding to each order of reflection are obtained. Then, the numerical relationship between different times of arrival and corresponding multipath types in the scene is studied. This, combined with an improved ellipse-cross-localization method, is used to determine the target position. Finally, numerical simulation results demonstrate that the proposed multi-target localization method effectively establishes the correlation between times of arrival and multipath types, enabling accurate localization of multiple targets in NLOS areas.

Keywords. Multipath correlation, non-line-of-sight (NLOS), time of arrival (TOA), ellipse-cross-localization, echo

1. Introduction

With the rapid development of intelligent applications, there is an increasingly urgent demand for target localization within various environments. However, in practical scenarios, targets are often obstructed by buildings, preventing electromagnetic waves from reaching the target through a line-of-sight (LOS) path, thereby rendering traditional detection methods inadequate [1], [2], [3], [4]. In an urban environment, multipath signals formed by reflection and diffraction of the building surface can compensate for the absence of an LOS path and enhance target perception capabilities. Therefore, researching the exploitation of signal multipath effects in non-line-of-sight (NLOS) environments to detect occluded targets is of great significance [5], [6], [7].

Recently, extensive studies have been conducted on exploiting the multipath effects of signals to detect occluded targets. In [8], researchers employed short-time Fourier transform techniques to extract Doppler signals from targets located behind corners, proposing a rapid algorithm for NLOS target detection. Expanding on this, Gustafsson et al. [9] conducted tests on a moving target in the actual scene and successfully realized

[1] Corresponding Author: Yishuo WU, 2123896753@qq.com.

the trajectory detection of the moving target by constructing the multipath propagation model of the scene and processing the echo signal by using background elimination and Doppler filtering technologies. However, the aforementioned studies only confirm the presence of targets in the environment without completing target localization. Zetik et al. [10] utilized wall reflections of echo signals and achieved one-dimensional localization of moving targets in corridors using UWB radar. To acquire two-dimensional positional information on targets, Zetik et al. [11] analyzed the diffraction phenomenon of signals occurring at building corners. Through the partitioning of the target area and integration of the diffraction path with the reflection path, they achieved two-dimensional target localization. However, when only single-path information is available, the accuracy of this method rapidly decreases. Du et al. [12] proposed a grid-matching target localization algorithm based on the principles of back-projection (BP) imaging. The algorithm selects the discrete grid with the highest matching degree as the target location, but variations in the matching threshold can lead to ambiguous target positions. To address the issue of multi-target localization, Li et al. [13], [14] established the symmetric relationship between the first-order ghost of the target and its real position. They employed a BP imaging algorithm to produce ghost images of the targets, and subsequently calculated matching factors, thereby determining the actual target positions using the principle of mirror reflection. Wu et al. [15] similarly utilized the geometric relationship between multipath ghost points to achieve joint estimation of target location and building layout. However, the imaging algorithm mentioned above, based on multipath superposition, may result in the aggregation of clutter energy, leading to the generation of more false target ghost points, which in turn affects the accurate determination of the target's actual position.

To address the issue of false points interfering with target location in the multipath imaging algorithm, this paper investigates the correlation between times of arrival (TOAs) and multipath types in multipath environments, proposing a novel NLOS multiple-target localization method. Firstly, the multipath propagation model formed by the reflection and diffraction of electromagnetic wave signals in an L-shaped building scenario is established. Then, the numerical relationship between the diffraction path, reflection path, and the combined path is analyzed to establish an effective correlation between the times of arrival and multipath types, thereby enabling the estimated target positions. Finally, electromagnetic simulation software is used to construct environment models and generate simulation data. Simulation results show that the proposed method can achieve accurate positioning of multiple targets.

2. Multipath Model

Consider an L-shaped corner scenario consisting of multiple walls, as shown in Figure 1. Wall-1 intersects perpendicularly with Wall-3 at the corner $\boldsymbol{C}=[x_c, y_c]$, and the distance between Wall-1 and Wall-2 is denoted as L. The radar is positioned on the side of Wall-3, and the target is located behind the corner, with coordinates $\boldsymbol{R}=[x_r, y_r]$ and $\boldsymbol{T}=[x_t, y_t]$ respectively.

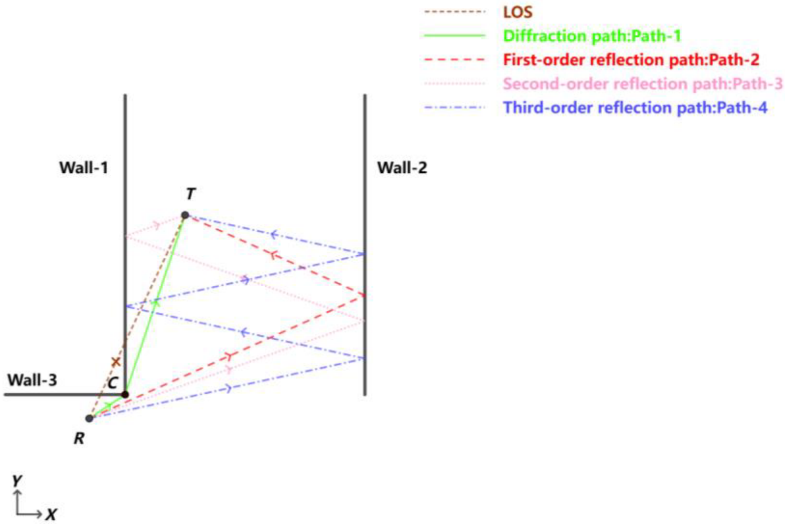

Figure 1. Multipath propagation model.

In the scenario depicted in Figure 1, the shielding of the building prevents the electromagnetic wave signal from propagating to the target through the LOS path. To achieve the occlusion target location, it is necessary to leverage the multipath signals generated by diffraction and multiple reflections of building surfaces. Studies have shown that reflections beyond the fourth order can cause significant attenuation of electromagnetic wave signal intensity, making it difficult to extract useful information from the echo signals [16], [17], [18]. Therefore, only four one-way signal propagation paths are considered in this paper, namely, the signal can reach the target through a diffraction path, first-order reflection path, second-order reflection path, and third-order reflection path.

When the radar transmits a pulse signal $s(t)$, the signal received by the radar is the echo superposition of the diffraction path and multiple reflection paths, which can be expressed as:

$$y(t) = \sum_{i=1}^{4}\sum_{j=1}^{4}\alpha_{ij}s(t-\tau_i-\tau_j)+\xi(t) \tag{1}$$

Where α_{ij} denotes the propagation path loss along different round-trip paths, while $\xi(t)$ denotes the environmental noise. τ_i and τ_j represent the propagation delay of the transmit paths and receive paths respectively, which can be calculated from known environment layout information.

The diffraction paths delay is given by:

$$\tau_i = \tau_j = \frac{\|\boldsymbol{RC}\|_2 + \|\boldsymbol{CT}\|_2}{c}, i = j = 1 \tag{2}$$

Where $\|\square\|_2$ represents the Euclidean distance, c denotes the propagation speed of the electromagnetic wave in vacuum. According to the principle of mirror reflection, the reflection of the signal about Wall-2 forms an alternative target-radar layout, resulting in a virtual radar position coordinate corresponding to the reflection path $path-p, p \in \{2,3,4\}$. Specifically, the coordinates of the virtual radar can be calculated by:

$$\begin{cases} \boldsymbol{R}_2 = (2x_c + 2L - x_r, y_r) \\ \boldsymbol{R}_3 = (x_r - 2L, y_r) \\ \boldsymbol{R}_4 = (2x_c + 4L - x_r, y_r) \end{cases} \tag{3}$$

Then, the reflection paths propagation delay can be calculated by:

$$\tau_i = \tau_j = \frac{\|\boldsymbol{R}_p \boldsymbol{T}\|_2}{c}, i, j, p \in \{2,3,4\} \tag{4}$$

3. The Proposed Algorithm

3.1. Multipath Assignment

From the view of the scene layout, the multipath echo should contain ten round-trip propagation paths. Due to noise and interference between signals, the actual number of TOA extracted may differ from the theoretical number. The extracted TOAs are saved in ascending order in the time vector $\boldsymbol{\tau}$, which can be expressed as:

$$\boldsymbol{\tau} = [\tau_1, \tau_2, \cdots, \tau_q, \cdots, \tau_Q], \tau_q < \tau_{q+1}, q = 1, 2, \cdots, Q-1 \tag{5}$$

Where τ_1 represents the time of arrival of the round-trip diffraction path echo. To associate the remaining TOAs in the equation with the corresponding echo types, utilizing the information that the sum of the round-trip time of arrival of the round-trip reflection path formed by the same reflection path and the round-trip diffraction path arrival time should be twice the arrival time of the combined diffraction and reflection path, a time cost function $\boldsymbol{\tau}_{\cos t}$ is defined. $\boldsymbol{\tau}_{\cos t}$ can be formed as:

$$\begin{aligned} \boldsymbol{\tau}_{\cos t} = sort\{[&\tau_1 + \tau_3 - 2\tau_2, \tau_1 + \tau_4 - 2\tau_2, \cdots, \tau_1 + \tau_Q - 2\tau_2, \cdots, \\ &\tau_1 + \tau_\beta - 2\tau_\alpha, \cdots, \tau_1 + \tau_Q - 2\tau_{Q-1}]\}, 1 \le \alpha < \beta \le Q-1 \end{aligned} \tag{6}$$

Where $sort\{\square\}$ represents arranging elements in ascending order. The combinations of TOAs corresponding to elements in the time cost function are defined as the matching cost vector $\boldsymbol{\tau}^{(m)} = (\tau_\alpha^{(m)}, \tau_\beta^{(m)})$, where $\tau_\alpha^{(m)}$ and $\tau_\beta^{(m)}$ are the TOAs corresponding to the m^{th} element in the time cost function. In theory, the times of arrival of the matching cost vector corresponding to the top elements in the time cost function are the TOAs of the round-trip reflection path and the diffraction path combined with the reflection path (the number of matching cost vectors extracted depends on the number of multipath types involved in the localization process). Consequently, the correct correlation between the times of arrival and multipath types can be realized by the TOA value size.

3.2. Target Localization

The principle of determining the target position using a diffraction path and various reflection paths is illustrated in Figure 2. The method assumes the ability to extract the TOAs of five paths from the environment: round-trip diffraction paths, round-trip first-order reflection path, round-trip second-order reflection path, diffraction path combined with first-order reflection path, and diffraction path combined with second-order reflection path. Subsequently, the electromagnetic wave signal propagation along the same or different transmitting and receiving paths is equivalent to a monostatic or bistatic localization system. Based on the results of the correlation between the times of arrival and the multipath types, the ellipse-cross-localization method [19], [20] is used to obtain the target position.

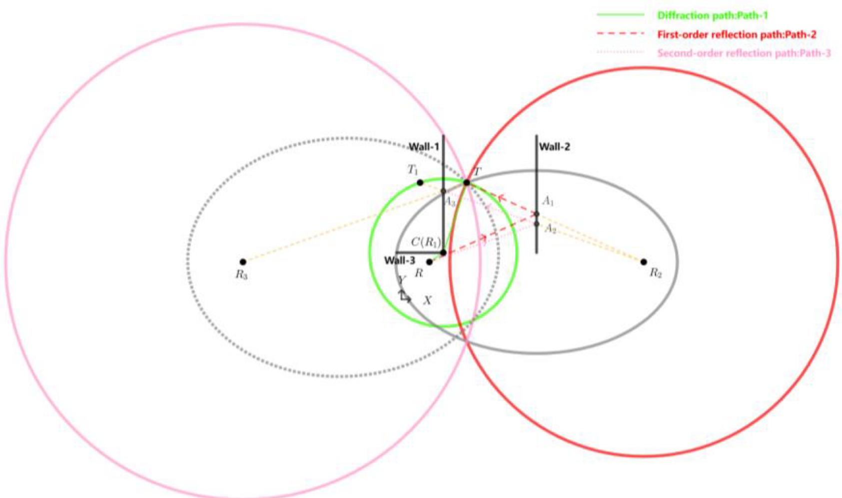

Figure 2. Principles of diffraction- and reflection-based localization.

However, when there is interaction between target-target and target-clutter, false TOA information is generated in the time vector, resulting in a matching cost vector value smaller than the value of the actual time of arrival combination. This leads to erroneous associations between the times of arrival and multipath types. Therefore, the following algorithm is introduced to adjust the associations.

After acquiring the time cost function, the target position is estimated by integrating the improved ellipse-cross-localization method. This approach guarantees an effective correlation between times of arrival and multipath types, leading to more precise target estimation outcomes. First, the two smallest matching cost vectors are selected from the time cost vector. Then, based on the numerical values of the times of arrival and their corresponding multipath types, they are correlated and jointly stored with the time of arrival of the round-trip diffraction path in the candidate time vector $\boldsymbol{D}$:

$$\boldsymbol{D} = [d_1, d_2, d_3, d_4, d_5] \tag{7}$$

Following the aforementioned correlation results, a set of candidate target positions is obtained using the ellipse-cross-localization method. The average of all candidate points is chosen as the estimated target position, denoted as $\tilde{\boldsymbol{T}}$. Subsequently, the time of arrival information when the target is located $\tilde{\boldsymbol{T}}$ is calculated and stored in the candidate time vector $\boldsymbol{\tau}^{real}$:

$$\boldsymbol{\tau}^{real} = [\tau_1^{real}, \tau_2^{real}, \cdots, \tau_{10}^{real}] \tag{8}$$

To evaluate the matching degree between $\boldsymbol{\tau}$ and $\boldsymbol{\tau}^{real}$, set the delay-matching vector $\boldsymbol{A}_a$:

$$\boldsymbol{A}_a = [A_1^a, A_2^a, \cdots, A_k^a, \cdots, A_{10}^a], a = 1,2,3,4,5 \tag{9}$$

where A_k^a can be calculated by:

$$A_k^a = \left| d_a - \tau_k^{real} \right|, d_a \in \boldsymbol{D}, \tau_k^{real} \in \boldsymbol{\tau}^{real} \tag{10}$$

Then reconstruct the elements in the delay matching vector $\boldsymbol{A}_a$:

$$A_k^a = \begin{cases} 1, \left| d_a - \tau_k^{real} \right| \le \Delta \\ 0, \left| d_a - \tau_k^{real} \right| > \Delta \end{cases} \tag{11}$$

Where Δ represents the correlation threshold. If the element in the delay matching vector $\boldsymbol{A}_a$ is less than the given threshold, it indicates that the theoretical multipath TOAs can be accurately correlated with the TOAs in the candidate time vector $\boldsymbol{D}$. The total number of correctly associated delays is expressed as $\boldsymbol{P}$:

$$\boldsymbol{P} = \sum_{a=1}^{5} sum(\boldsymbol{A}_a) \tag{12}$$

Where $sum(\boldsymbol{A}_a)$ represents the sum of all elements in $\boldsymbol{A}_a$. When the total number of correctly associated delays is consistent with the total number of TOA used for localization, it indicates that the times of arrival are correctly associated with the multipath types, and the estimated target $\tilde{\boldsymbol{T}}$ is considered the result of target estimation. If they do not match, the minimum number of selected matching cost vectors is increased, repeating the above steps until the total number of correctly associated delays matches the total number of TOA used for estimation.

With an increase in the number of targets in the scene, improvement in the method for multiple targets localization can be achieved by setting an appropriate path threshold

ε. The detailed procedure of the proposed NLOS multiple targets localization method is summarized in Algorithm 1.

Algorithm 1 NLOS Multiple Targets Localization

Input: $\boldsymbol{\tau}$, Δ, ε

Output: $\tilde{\boldsymbol{T}}_K$

Initialization: $\tilde{\boldsymbol{T}}_K$ $\tilde{\boldsymbol{\tau}} = \boldsymbol{\tau}$, $K = 0$, $num = 2$

Count the elements in $\tilde{\boldsymbol{\tau}}$: l

while $l - \varepsilon * K > \varepsilon$ **do**

$num = num + 1$

Calculate $\tilde{\boldsymbol{\tau}}_{\cos t}$ using (6)

Select num smallest elements from $\tilde{\boldsymbol{\tau}}_{\cos t}$, store pair-to-pair combinations in candidate vector $\{\boldsymbol{D}_1, \boldsymbol{D}_2, \cdots, \boldsymbol{D}_n\}$

for $i = 1, 2, \cdots, n$ **do**

Use $\boldsymbol{D}_i$ to calculate

Calculate P using (9)-(12)

if $P > 4$ **then**

$K = K + 1$, $\tilde{\boldsymbol{\tau}} = \tilde{\boldsymbol{\tau}}\{-\}\boldsymbol{D}$, l, $num = 2$

break

end if

end for

end while

4. Numerical Result

In this section, the numerical simulation is carried out to demonstrate the effectiveness of the proposed NLOS target localization algorithm.

The scene is set up as depicted in Figure 1. The coordinates of the corner in the scene are $\boldsymbol{C} = [x_c, y_c]$, and the width between Wall-1 and Wall-2 is 5m. The relative permittivity of the walls in the scene is set to 7, with a conductivity of 0.05 S/m. The target is represented by a cylinder with a relative permittivity of 55, conductivity of 1.05 S/m, and a radius of 0.2m. The transmitting signal of the radar is set to the Ricker wavelet signal, with a center frequency of 1.5GHz.

In the first simulation, the target position is $\boldsymbol{T} = (4.0, 6.0)$. The correlation between times of arrival and multipath types for localization results is illustrated in Figure 3. In Figure 3, the true target position is indicated by a blue square, while the candidate target positions are depicted as an orange circle. When the times of arrival are erroneously associated with the multipath types, as shown in Figures 3(a) and 3(b), the candidate points of the target location in the localization result exhibit a distinct scattered distribution, with only a few points distributed around the true target position. Under the incorrect correlation, the estimated target position is $\tilde{\boldsymbol{T}} = (2.6653, 6.7265)$, and the number of elements in the candidate time vector correctly associated with the times of arrival at this position is 0. Therefore, it is necessary to reassociate the times of arrival with the multipath types. When the times of arrival are correctly associated with the multipath types, as shown in Figures 3(c) and 3(d), the candidate points of the target location in the localization result are more concentrated, all located near the true target position. Under the correct correlation, the estimated target position is $\tilde{\boldsymbol{T}} = (3.9694, 5.9723)$, and the number of elements in the candidate time vector correctly associated with the times of arrival at this position is 5. Therefore, the target localization result is obtained as $\tilde{\boldsymbol{T}} = (3.9694, 5.9723)$.

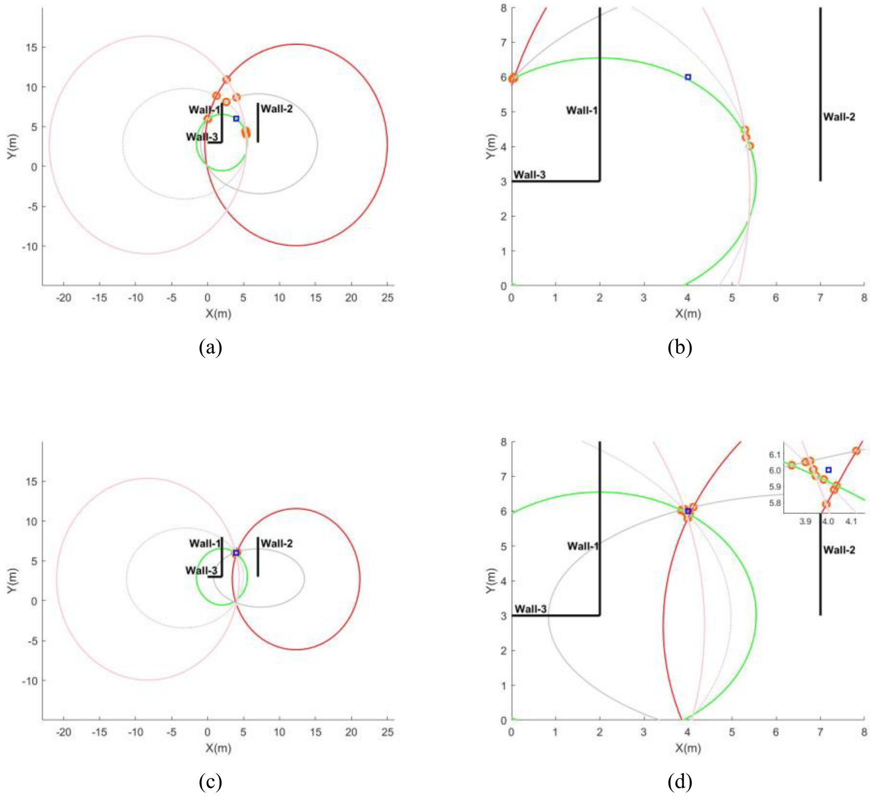

Figure 3. The single target correlation results, (a) erroneous correlation between times of arrival and multipath types, (b) local enlargement of erroneous correlation, (c) correct correlation between times of arrival and multipath types, (d) local enlargement of correct correlation.

To further evaluate the performance of the proposed algorithm, simulation experiments were conducted on targets at different positions, and the estimated target positions are shown in Table 1. It can be observed from the table that the estimated values of targets at different positions can match well with the true target values. The average localization error of the proposed NLOS target localization method is 4.3113 cm.

Table 1. Localization results

True target positions	(3.6,5.0)	(3.0,5.0)	(3.0,6.0)
Estimated target positions	(3.5618,4.9750)	(2.9672,4.9658)	(2.9739,5.9656)
True target positions	(3.0,5.5)	(4.0,6.5)	(3.3,5.5)
Estimated target positions	(2.9718,5.4659)	(3.9720,6.4701)	(3.2699,5.4695)
True target positions	(3.6,5.5)	(3.9,5.5)	(4.2,5.5)
Estimated target positions	(3.5683,5.4724)	(3.8667,5.4752)	(4.1649,5.4769)

In the second simulation, considering the presence of two targets in the scene, with target positions denoted as $\boldsymbol{T}_1 = (4.2, 5.5)$ and $\boldsymbol{T}_2 = (3.0, 5.5)$. By processing the time vector composed of the TOAs of the two targets using the NLOS target localization algorithm described in Section 3, the dual-target localization results associated with the correct multipath are obtained, as shown in Figure 4. In Figure 4, the blue square represents the true position of the target $\boldsymbol{T}_1$, and the purple square represents the true position of the target $\boldsymbol{T}_2$. The estimated positions of the two targets are $\boldsymbol{T}_1 = [4.1649, 5.4769]$ and $\boldsymbol{T}_2 = [2.9388, 5.4436]$ respectively, with both the horizontal and vertical coordinate errors concerning the true target positions being within two decimal places. Simulation results indicate that the proposed method maintains good localization performance even in scenarios with multiple targets in NLOS regions.

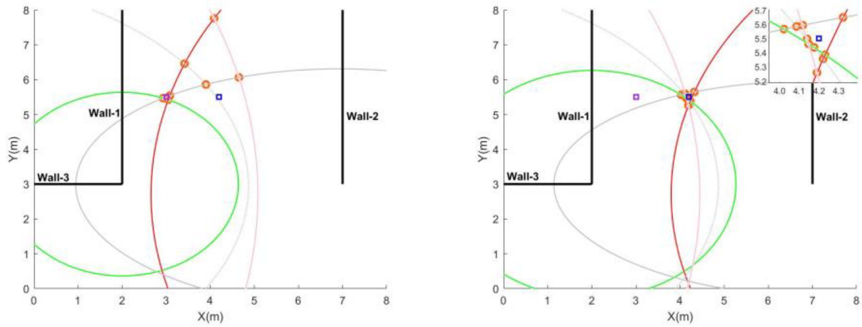

Figure 4. The two targets correlation results, (a) correct correlation between times of arrival of target $\boldsymbol{T}_2$ and multipath types, (b) correct correlation between times of arrival of target $\boldsymbol{T}_1$ and multipath types.

5. Conclusions

This paper proposes a method for localizing obscured targets using multipath echoes. Firstly, considering the known geometric layout information of buildings, a multipath signal propagation model in an L-shaped building scene is established. Then, by exploiting the correlation between times of arrival and multipath types, a fusion-matching-based ellipse-cross-localization method is proposed. Finally, numerical simulation results demonstrate that the proposed method can achieve accurate target localization in scenarios with single or multiple targets, validating the effectiveness of the proposed approach.

The research in this paper did not take into account the possibility of missing some multipath information in practical scenarios. Therefore, to enhance the robustness of the proposed method, future research could further utilize multipath parameters such as direction of departure (DOD) and direction of arrival (DOA) or improve the algorithm by introducing target trackers.

References

[1] S. Xia, Y. Xiang, K. Xiong, S. Guo, and G. Cui, "A radar target tracking algorithm based on learning displacement," IEEE Geosci. Remote Sensing Lett. vol. 21, pp. 1–5, 2024.

[2] Y. Liang and H. Li, "LOS signal identification for passive multi-target localization in multipath environments," IEEE Signal Process. Lett. vol. 30, pp. 1597–1601, 2023.

[3] R. Feng, E. De Greef, M. Rykunov, H. Sahli, S. Pollin, and A. Bourdoux, "Multipath ghost classification for MIMO radar using deep neural networks," in 2022 IEEE Radar Conference (RadarConf22), New York City, NY, USA, pp. 1–6, Mar. 2022.

[4] K. Han and S. Hong, "Detection and localization of multiple humans based on curve length of I/Q signal trajectory using MIMO FMCW radar," IEEE Microwave and Wireless Components Letters, vol. 31, no. 4, 2021.

[5] P. Setlur, T. Negishi, N. Devroye, and D. Erricolo, "Multipath exploitation in non-LOS urban synthetic aperture radar," IEEE J. Sel. Top. Signal Process, vol. 8, no. 1, pp. 137–152, Feb. 2014.

[6] Y. Shen, M. Zhang, Y. Wu, G. Cui, and S. Guo, "Darting-out target detection with NLOS signals for vehicle MIMO mmWave radar," in 2023 IEEE Radar Conference (RadarConf23), San Antonio, TX, USA, pp. 1–6, May. 2023.

[7] J. Chen, Y. Zhang, S. Guo, G. Cui, P. Wu, C. Jia, et al., "Joint estimation of NLOS building layout and targets via sparsity-driven approach," IEEE Trans. Geosci. Remote Sensing, vol. 60, pp. 1–13, 2022.

[8] A. Sume, M. Gustafsson, M. Herberthson, A. Janis, S. Nilsson, J. Rahm, et al., "Radar Detection of Moving Targets Behind Corners," IEEE Trans. Geosci. Remote Sensing, vol. 49, no. 6, pp. 2259–2267, Jun. 2011.

[9] M. Gustafsson, A. Andersson, T. Johansson, S. Nilsson, A. Sume, and A. Orbom, "Extraction of human micro-Doppler signature in an urban environment using a 'sensing-behind-the-corner' radar," IEEE Geosci. Remote Sensing Lett, vol. 13, no. 2, pp. 187–191, Feb. 2016.

[10] R. Zetik, M. Roding, and R. S. Thoma, "UWB localization of moving targets in shadowed regions," in 2012 6th European Conference on Antennas and Propagation (EUCAP), Prague, Czech Republic, pp. 1729–1732. Mar. 2012.

[11] R. Zetik, M. Eschrich, S. Jovanoska, and R. S. Thoma, "Looking behind a corner using multipath-exploiting UWB radar," IEEE Trans. Aerosp. Electron. Syst., vol. 51, no. 3, pp. 1916–1926, Jul. 2015.

[12] H. Du, C. Fan, C. Cao, Z. Chen, and X. Huang, "NLOS target localization behind an L-shaped corner based on grid matching," in IET International Radar Conference (IET IRC 2020), Online Conference, pp. 1066–1071. 2021.

[13] S. Guo, S. Li, G. Cui, S. Fan, L. Kong, and X. Yang, "MIMO radar localization of targets behind L-shaped corners," in 2020 IEEE 11th Sensor Array and Multichannel Signal Processing Workshop (SAM), Hangzhou, China, pp. 1–4. Jun. 2020.

[14] S. Li, S. Guo, J. Chen, X. Yang, S. Fan, C. Jia, et al., "Multiple targets localization behind L-shaped corner via UWB radar," IEEE Trans. Veh. Technol., vol. 70, no. 4, pp. 3087–3100, Apr. 2021.

[15] P. Wu, J. Chen, S. Guo, G. Cui, L. Kong, and X. Yang, "NLOS positioning for building layout and target based on association and hypothesis method," IEEE Trans. Geosci. Remote Sensing, vol. 61, pp. 1–13, 2023.

[16] H. Du, C. Fan, Z. Chen, C. Cao, and X. Huang, "NLOS target localization with an L-band UWB radar via grid matching," PIER M, vol. 97, pp. 45–56, 2020.

[17] S. Xue, S. Guo, P. Wu, J. Chen, Z. Xu, and G. Cui, "NLOS target localization method in long L-shaped scenario with SISO UWB radar," in 2023 3rd International Conference on Frontiers of Electronics, Information and Computation Technologies (ICFEICT), Yangzhou, China, pp. 525–530. May. 2023.

[18] S. Fan, Y. Wang, G. Cui, S. Li, S. Guo, M. Wang, et al., "Moving target localization behind L-shaped corner with a UWB radar," in 2019 IEEE Radar Conference (RadarConf), Boston, MA, USA, pp. 1–5. Apr. 2019.

[19] X. Huang, G. Cui, S. Guo, L. Kong, and X. Yang, "A novel noncoherent localization approach for through-the-wall radar," in 2017 IEEE Radar Conference (Radar Conf), Seattle, WA, USA, pp. 1245–1249. May 2017.

[20] X. Yang, S. Fan, S. Guo, S. Li, G. Cui, and W. Zhang, "NLOS target localization behind an L-shaped corner with an L-band UWB radar," IEEE Access, vol. 8, pp. 31270–31286, 2020.